

This article was published in an Elsevier journal. The attached copy is furnished to the author for non-commercial research and education use, including for instruction at the author's institution, sharing with colleagues and providing to institution administration.

Other uses, including reproduction and distribution, or selling or licensing copies, or posting to personal, institutional or third party websites are prohibited.

In most cases authors are permitted to post their version of the article (e.g. in Word or Tex form) to their personal website or institutional repository. Authors requiring further information regarding Elsevier's archiving and manuscript policies are encouraged to visit:

<http://www.elsevier.com/copyright>



NMR studies and DFT calculations of the symmetric intramolecular NHN-hydrogen bond of bis-(2-pyridyl)-acetonitrile: Isotope labeling strategy for the indirect ^{13}C -detection of $^{15}\text{N}^{15}\text{N}$ couplings

Mariusz Pietrzak ^{a,c}, Claudia Benedict ^a, Holger Gehring ^b, Ewald Daltrozzi ^b,
Hans-Heinrich Limbach ^{a,*}

^a Institut für Chemie und Biochemie der Freien Universität Berlin, Takustraße 3, D-14195 Berlin, Germany

^b Fachbereich Chemie, Universität Konstanz, Fach M 739, D-78457 Konstanz, Germany

^c Institute of Physical Chemistry, Polish Academy of Sciences, Kasprzaka 44/52, 01-224 Warszawa, Poland

Received 1 March 2007; received in revised form 16 April 2007; accepted 16 April 2007

Available online 22 April 2007

Dedicated to Prof. Lucjan Sobczyk on the occasion of his 80th birthday.

Abstract

The ^1H , ^{15}N , and ^{13}C NMR spectra of partially ^{15}N labeled bis-(2-pyridyl)-acetonitrile (**1**) dissolved in CDCl_3 and CD_2Cl_2 have been measured in order to characterize its intramolecular NHN hydrogen bond. A fast proton tautomerism renders the molecule symmetric within the NMR timescale which complicates the determination of the scalar coupling constant $^{2h}J(^{15}\text{N}, ^{15}\text{N}) \equiv J(\text{N}, \text{N})$ across the intramolecular NHN-hydrogen bond. It is shown that an isotopic labeling scheme where experiments are performed on a mixture of $1\text{-}^{14}\text{N}^{14}\text{N}$, $1\text{-}^{14}\text{N}^{15}\text{N}$, and $1\text{-}^{15}\text{N}^{15}\text{N}$ facilitates the direct determination of $J(\text{N}, \text{N})$ from the non-decoupled ^{15}N NMR spectra as well as the indirect detection via ^{13}C NMR. Thus, a value of $J(\text{N}, \text{N}) = 10.3 \pm 0.5$ Hz is obtained, which is similar to the corresponding value of 10.6 ± 0.5 Hz found previously for the seven-membered H-chelate *N,N'*-diphenyl-6-aminopentafulvene-1-alimine- $^{15}\text{N}_2$ (**2**). By contrast, the crystallographic N...N distances and hydrogen bond angles of both compounds are very different, i.e. 2.65 Å and about 140° in the case of **1** and 2.79 Å and about 160° in the case of **2**. However, the sum of the calculated NH and H...N distances is the same for both compounds, i.e. 2.75 Å. This finding supports the previous proposition that the values of $J(\text{A}, \text{B})$ of a hydrogen bond AHB are correlated with the sum of the two hydrogen – heavy atom distances rather than with the heavy atom distance.

© 2007 Elsevier B.V. All rights reserved.

Keywords: NMR; ^1H NMR; ^{15}N NMR; ^{13}C NMR; Hydrogen bond; $^{2h}J(\text{N}, \text{N})$; $^{1h}J(\text{N}, \text{H})$; 6-Aminofulvene-1-aldimines

1. Introduction

The discovery of scalar nuclear coupling constants across OH^{15}N hydrogen bonds [1], across $^{19}\text{FH}^{19}\text{F}$ hydrogen bonds [2], and across $^{15}\text{NH}^{15}\text{N}$ hydrogen bonds [3,4] has stimulated a number of experimental and theoretical studies. Scalar one-bond HB and two-bond AB couplings of hydrogen bridges $\text{A}-\text{H}\cdots\text{B}$ provide information about the geometries and hence electrostatic properties of hydro-

gen bridges [5], whereas long-range couplings involving remote heavy atom nuclei such as ^{13}C , ^{31}P are generally important to establish hydrogen bond contacts in biomolecules. As scalar couplings to ^{17}O have not yet been observed because of electrical quadrupole effects, $^{15}\text{N}-\text{H}\cdots^{15}\text{N}$ hydrogen bonds are of special interest as they can form functional hydrogen bonds in biomolecules. An account of quantum-mechanical calculations of all scalar coupling constants in this type of system has been published recently [6]. Various structural features determine the $^{15}\text{N}, ^{15}\text{N}$ coupling constants, which we write in this paper as $^{2h}J(^{15}\text{N}, ^{15}\text{N}) \equiv ^{2h}J(\text{N}, \text{N}) \equiv J(\text{N}, \text{N})$. The most

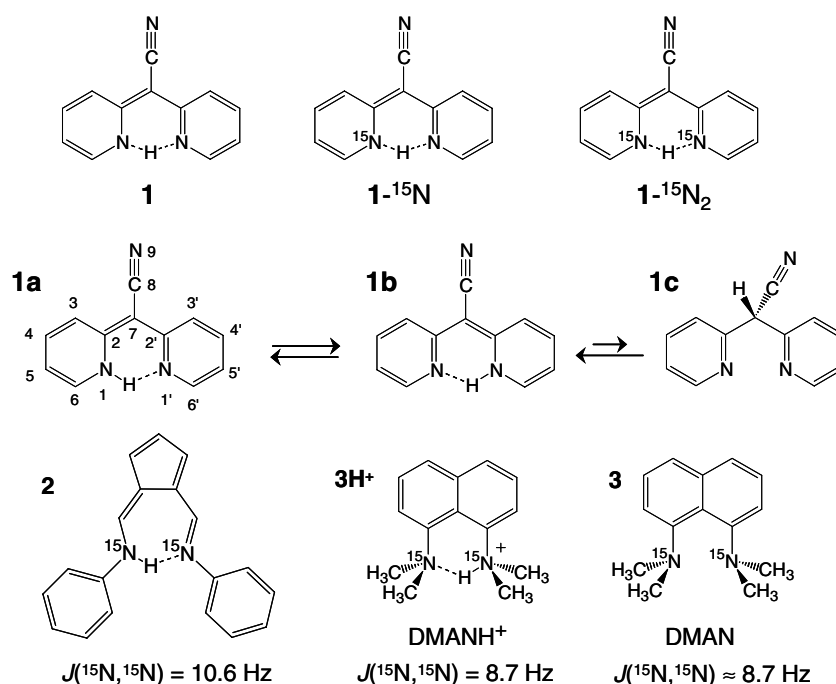
* Corresponding author. Tel.: +49 3083855375; fax: +49 3083855310.
E-mail address: limbach@chemie.fu-berlin.de (H.-H. Limbach).

important parameter is the N...N distance. When the $^{15}\text{N}\dots\text{H}$ distances are increased, the coupling constant $J(\text{N},\text{H})$ decreases, becomes zero, changes sign and only finally vanishes, as has been found previously [7,8], in a similar way as found before for related FHF-hydrogen bonds [5]. This sign change has been confirmed recently [6].

Unfortunately, scalar couplings across hydrogen bonds can be observed only in the slow hydrogen bond exchange regime. Thus, small molecules with intermolecular hydrogen bonds reveal these couplings only at low temperatures [2,5,9,10], whereas hydrogen bonds in biomolecules [3,11–17] can be often observed at room temperature. The same is true for small molecules containing intramolecular hydrogen bonds. Here, it is, however, necessary to establish that the observed couplings are not the result of a coupling pathway along the molecular backbone. This was achieved in the case of the well-known protonated proton sponge 1,8-bis(dimethylamino)-naphthalene- H^+ (DMANH $^+$) by comparison with the unprotonated compound (Scheme 1) [18]. Another problem of intramolecular $^{15}\text{N}-\text{H}\dots^{15}\text{N}$ hydrogen bonds can be a fast proton tautomerism in symmetrically substituted molecules which renders the two nitrogen atoms equivalent. Often it is not easy to elucidate whether the proton moves in a double or single well potential. For example, the case of DMANH $^+$ (3H^+) has been studied recently experimentally and theoretically by Sobczyk et al. [19]. The question arises whether the measurement of $^{15}\text{N}\dots^{15}\text{N}$ coupling constants provides a solution to this problem. Because of the molecular symmetry these couplings can not be measured directly. However, in the case of $^{13}\text{C}-^{13}\text{C}$ scalar couplings between chemically equivalent carbon atoms it has been shown that these couplings

can be measured indirectly if the carbon atoms form a high-order spin system with coupled protons [20]. Some of us have proposed to use a similar method for the detection of scalar $^{15}\text{N}\dots^{15}\text{N}$ couplings in **2** and 3H^+ by analysis of the signals of coupled ^{13}C nuclei at natural abundance [8,18], where the nuclei $^{13}\text{C}-^{15}\text{N}-^{15}\text{N}-^{12}\text{C}$ form high-order spin systems of the ABX type. The chemical equivalence between the two nitrogen atoms A and B is lifted by $^{13}\text{C}/^{12}\text{C}$ isotope effects which also increases the number of parameters which need to be extracted from the spectra, in contrast to a fully labeled four-spin system $^{13}\text{C}-^{15}\text{N}-^{15}\text{N}-^{13}\text{C}$ of the AA'XX' type, which is, however, very difficult to synthesize. Measurements at different magnetic fields can help to increase the reliability of the values detected [8,18], but are not compulsory as has been shown in the case of proton sponges [21]. Here, we show that measurements of a mixture of partially doubly and singly ^{15}N labeled isotopologs can assist the detection of the desired $^{15}\text{N}\dots^{15}\text{N}$ coupling constants.

The system which we have chosen to study is bis-(2-pyridyl)-acetonitrile (**1**, Scheme 1) which contains an intramolecular N—H...N hydrogen bond as a part of a six-membered H-chelate. **1** is known for a long time [22]. The electronic coupling between the two pyridine rings and the hydrogen bond lead to a preferred planar structure and a yellow colour which has been studied using UV/VIS and fluorescence methods [23]. The standard ^1H and ^{13}C NMR data [24] show that both pyridine rings are equivalent in the NMR time scale as depicted in Scheme 1. For the H-chelate structure of **1** the double vs. single well question was – as for all comparable, symmetrical hydrogen chelates – undoubtedly solved in favor of a double well



Scheme 1. Structure of bis-(2-pyridyl)-acetonitrile (**1**) and its tautomeric equilibrium. Structures of N,N' -diphenyl-6-aminopentafulvene-1-alimine (**2**) [8] and of 1,8-bis(dimethylamino)naphthalene (**3**) [18].

potential by UV/VIS spectroscopic evidence [25,26]. The proton signal at low field (16.3 ppm) indicates strong N—H...N hydrogen bond, which is also indicated in the IR spectra by a very broad band around 2750 cm⁻¹ and a double band with significantly smaller half-widths at 2358 and 2341 cm⁻¹ for the corresponding N—D...N – absorptions in the deuterated compound [25].

We chose **1** for comparison with DMANH⁺ (3H⁺) and *N,N'*-diphenyl-6-aminopentafulvene-1-alimine-¹⁵N₂ (**2**, Scheme 1) for which two-bond N,N coupling constants of 8.7 and of 10.6 Hz were observed. This is of the same order as the two-bond coupling constants across ¹⁵N—H...¹⁵N hydrogen bonds in Watson–Crick nucleic acid base pairs [11]. In order to elucidate a correlation of *J*(N,N) with the hydrogen bond geometries it would have been desirable to know the neutron crystal structure of **1**. Unfortunately, even the X-ray structure of the latter is unknown, in contrast to three symmetrically substituted derivatives which exhibit the N...N distances of about 2.65 Å [24,27,28]. This value is substantially smaller than the corresponding distance of 2.79 Å found for compound **2** [29]. The N—H...N angle and the NH-distances cannot be determined correctly by X-ray studies, because of well-documented difficulties in locating the hydrogen atom [30]. Therefore, we decided to conduct DFT calculations at a high level of theory (B3PW91/631+G**) which have been shown to provide reasonable estimates of H-bond geometries [31].

This paper is organized as follows. After an experimental section the results are presented and discussed.

2. Experimental section

The synthesis of partially ¹⁵N labeled bis-(2-pyridyl)-acetonitrile (**1**) was done in two stages. In the first stage, ¹⁵N labeled 2-pyridone (**4**) was prepared in four steps according to the procedure of Stetten et al. from coumalic acid and ¹⁵NH₄Cl (¹⁵N fraction about 95%, Chemotrade, Leipzig) [32]. In the second stage, **4** was converted into **1** as outlined in Scheme 2. Firstly, 2-Cl-pyridone (**5**) was prepared from **4** according to Saidova et al. [33], **5** was then converted into **7** according to Borrer et al. [34]. Finally, **1** was prepared from **5** and **7** according to the standard method (DMF/NaH

as reaction media), which was developed as a general route to both symmetrical and unsymmetrical hydrogen chelates of any nitrogen heterocycle [35].

In order to obtain a partial enrichment, a mixture of ¹⁵N labeled and non-labeled **4** was used as the starting material.

The ¹H, ¹³C{¹H}, ¹⁵N{¹H}, and ¹⁵N measurements described below were done on a Bruker AMX 500 instrument operating at 500.13 MHz for ¹H, at 125.76 MHz for ¹³C, and at 50.70 MHz for ¹⁵N. Experiments were done in the temperature region between 183 and 213 K in order to suppress residual intermolecular proton exchange which broadens the NMR signals. Additional ¹H NMR experiments were performed using a JEOL JNM-GX 400 FT-NMR spectrometer working at 400 MHz. As solvents we used CDCl₃, CD₂Cl₂, and DMSO-*d*₆. The sample concentrations were about 0.2 M.

For the simulation of high-order NMR spectra, a special computer program was written using Matlab[®] as a programming language.

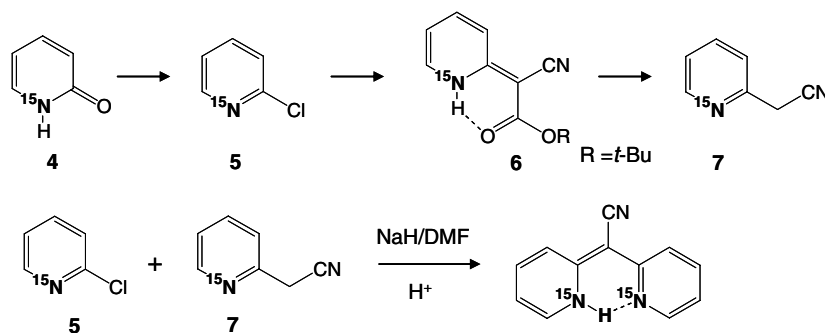
3. Results

The results of the NMR measurements of various isotopologs of **1** containing either zero, one, or two ¹⁵N nuclei dissolved in various solvents and done at different temperatures are summarized in Tables 1–3. Some H/D isotope effects on chemical shifts are included. Two forms are observed which are in slow exchange with each other even at elevated temperature, i.e. **1a/1b** and **1c** (Scheme 1). The NMR parameters of **1a/1b** are assembled in Tables 1 and 2, and those of **1c** in Table 3. The assignment of all signals was straightforward and confirmed by ¹³C and ¹⁵N measurements of the labeled compounds.

Because of the fast tautomeric equilibrium between **1a** and **1b** all NMR parameters of these species represent averages over both forms which are degenerate in the absence of asymmetric isotopic substitution, i.e.

$$\delta_i = \frac{1}{2}(\delta_i(a) + \delta_i(b)), \quad J_{ij} = \frac{1}{2}(J_{ij}(a) + J_{ij}(b)). \quad (1)$$

In the presence of asymmetric substitution, i.e. in natural abundance ¹³C spectroscopy and in the singly ¹⁵N labeled isotopolog this equation is also valid in very good approximation, as heavy atom equilibrium isotope effects are small.



Scheme 2. Synthesis of the ¹⁵N labeled bis-(2-pyridyl)-acetonitrile (**1**) from the ¹⁵N labeled 2-pyridon (**7**) obtained according to [32c–e].

Table 1
NMR chemical shifts of **1a/1b**

Solvent: T/K:	δ/ppm							
	CDCl ₃ 213	CDCl ₃ 298	CD ₂ Cl ₂ 183	CD ₂ Cl ₂ 233	CD ₂ Cl ₂ RT	DMSO- <i>d</i> ₆ 304	Acetone- <i>d</i> ₆ 295	CD ₃ OD 295
H1	16.28 (35 Hz) ^a	16.29 (140 Hz) ^a	16.27 (12 Hz) ^a	16.26	16.25 (93 Hz) ^a	15.79	16.1	–
H3	7.40	7.40	7.27	7.30	7.35	7.21	7.29	7.27
H4	7.53	7.48	7.49	7.50	7.50	7.64	7.62	7.57
H5	6.68	6.62	6.64	6.64	6.64	6.75	6.72	6.70
H6	7.97	7.92	7.95	7.96	7.95	8.17	8.11	8.08
C2	155.2		154.5					
C3	119.4		118.7					
C4	136.3		136.4					
C5	112.7		112.5					
C6	139.2		139.3					
C7	67.7		66.2					
C8	122.2		122.2					
N1	–168.9 ^b	–169.4 ^b	–168.7 ^b					
N1	–169.5 ^c	–169.9 ^c	–169.4 ^c					

^a Half-width *W* of each exchange broadened ¹H–¹⁵N doublet or of coalesced doublet.

^b ¹⁵N₂ isotopolog.

^c ¹⁴N¹⁵N isotopolog.

Table 2
NMR coupling constants *J* and H/D isotope effects Δ on chemical shifts of **1a/1b**

Solvent: T/K:	<i>J</i> /Hz			ⁿ ΔX(N)/ppb ^a
	CDCl ₃ 295	CD ₂ Cl ₂ 183	CDCl ₃ 213	CDCl ₃ 213
H1		¹ <i>J</i> (H1,N1) = 43		¹ ΔH1(N1) ≈ 0 ^b ΔH1(N1 + N1') ≈ 0 ^b
H3	³ <i>J</i> (H3,H4) = 8.6			
H4	³ <i>J</i> (H4,H5) = 7.0 ³ <i>J</i> (H3,H4) = 8.6			
H5	³ <i>J</i> (H5,H6) = 5.9 ³ <i>J</i> (H4,H5) = 7.0			
H6	³ <i>J</i> (H5,H6) = 5.9			
C2			¹ <i>J</i> (C2,N1) = 6.8 ³ <i>J</i> (C2,N1') = 1.3	¹ ΔC2(N1) = 33 ³ ΔC2(N1') = –18 ΔC2(N1 + N1') = 15
C3			¹ <i>J</i> (C3,H3) = 166.3	
C4			¹ <i>J</i> (C4,H4) = 163.2	
C5			¹ <i>J</i> (C5,H5) = 168.2	
C6			¹ <i>J</i> (C6,N1) = 7.8 ^{3h} <i>J</i> (C6,N1') ~ 0.5 ¹ <i>J</i> (C6,H6) = 179.0	¹ ΔC6(N1) = 61 ⁵ ΔC6(N1') = –47 ΔC6(N1 + N1') = 14
C7			² <i>J</i> (C7,N1) = 3.9	² ΔC7(N1) = 6.5 ΔC7(N1 + N1') = 13
C8			³ <i>J</i> (C8,N1) = 2.6	³ ΔC8(N1) = –1 ΔC8(N1 + N1') = –2
N1	¹ <i>J</i> (N1,H1) = 42 ¹ <i>J</i> (N1,H6) = 7	¹ <i>J</i> (N1,H1) = 43 ¹ <i>J</i> (N1,H6) ~ 6.5	<i>J</i>(N,N) = 10.3	⁴ ΔN1(N1') = –0.60 ppm

Bold values indicates most important parameters measured.

^a ⁿΔX(N) = δX(¹⁵N) – δX(¹⁴N) indicates the isotope effect on the chemical shift of X, caused by substitution of ¹⁴N by ¹⁵N in a nitrogen site at a distance of *n* bonds.

^b in CD₂Cl₂ at 183 K.

Table 3
NMR parameters of **1c**

	δ/ppm	J/Hz
Solvent:	DMSO- d_6	DMSO- d_6
ν_0/MHz :	400	400
T/K :	300	300
CH	6.02	$^1J(\text{H}3, \text{H}2) \approx 8$
H3	7.48	$^1J(\text{H}4, \text{H}5) \approx 7$
H4	7.85	$^1J(\text{H}5, \text{H}6) \approx 5$
H5	7.37	
H6	8.56	

3.1. ^1H NMR spectroscopy of **1**

The hydrogen bond proton of **1a/1b** exhibits a signal around 16.2 ppm. No substructure is observed at room temperature for the non-labeled compound. The line width is larger than 100 Hz, arising from intermolecular proton exchange. At lower temperatures the latter is quenched, but in the best case, at 183 K, using CD_2Cl_2 as solvent, still a line width of 12 Hz was observed. Potential changes of proton chemical shifts upon substitution with ^{15}N are in the range of experimental error. Whereas **1**- $^{14}\text{N}^{14}\text{N}$ gives rise to a singlet, because the scalar coupling to ^{14}N is suppressed by ^{14}N quadrupole relaxation, **1**- $^{15}\text{N}^{14}\text{N}$ contributes to a doublet split by 43 Hz and **1**- $^{15}\text{N}^{15}\text{N}$ to a triplet exhibiting the same ^1H – ^{15}N coupling constant. This value is typical for six-membered H-chelates [36].

As shown previously by UV/VIS spectroscopy [23,25], in spite of the π -conjugation and the additional stabilization of the coplanar H-chelate structure, at 298 K in solution the compound is subject to 180° flips of the pyridine moieties which are rapidly on the NMR time scale (rotation frequencies of about 10^3 s^{-1}). As all non-H-chelate rotamers, including the 180° rotated isomers are energetically highly unfavorable, neither at lower (methylene chloride, -90°C) nor higher (DMSO, 100°C) temperatures any line broadening can be observed, e.g. the rotamer equilibrium is so far on the side of the H-chelate form, that the rotation neither effects the line shapes nor the proton chemical shifts. Due to the mobility of the pyridines, the chelate proton undergoes rapid intermolecular exchange with the solvent (or the solvent's water content) and only at special conditions (lower temperatures and/or exclusion of water traces) the $^3J(\text{H}1, \text{H}6)$ can be observed.

If $J_{ij}(\text{a})$ in Eq. (1) represents the coupling of the H-chelate proton with a nitrogen or hydrogen atom in the same pyridine ring, $J_{ij}(\text{b})$ represents a value across the hydrogen bond. Neglecting the latter, it follows that the intrinsic values are app. twice the observed values. However, recently small positive values up to +4 Hz have been observed for such couplings across the NHN-hydrogen bonds of seven-membered H-chelates [8]. Thus, when the NH distance is increased and the proton shifted along the hydrogen bond, the intrinsic NH-coupling constant which is negative approaches zero, becomes positive and only then

decreases to zero [8]. Thus, the intrinsic value of 86 Hz for the intrinsic coupling constant $J(\text{H}1, \text{N}1)(\text{a})$ only represents an estimate. However, this value is in good agreement with comparable systems with fixed NH groups and similar NH-distances, exhibiting values between 88 and 92 Hz [37].

As mentioned above, in addition to the chelate forms **1a**, **1b**, small amounts of the non-conjugated isomer **1c** (Scheme 1) can be observed in the ^1H NMR spectra. At 298 K we found by NMR signal integration amounts of 2% in CDCl_3 and 3% in DMSO of **1c** in equilibrium with **1a**, **1b**. At 90°C in DMSO- d_6 , the equilibrium content of **1c** is risen up to 9%. From these data, for the equilibrium an enthalpy of about 16.1 kJ/mol can be estimated.

3.2. ^{15}N NMR spectroscopy of **1**

In Fig. 1a is depicted the superimposed experimental and calculated ^{15}N NMR spectrum of partially ^{15}N -labeled **1** dissolved in CD_2Cl_2 , recorded at 183 K without ^1H decoupling. In principle, we expect for each isotopologs **1**- $^{14}\text{N}^{15}\text{N}$ and **1**- $^{15}\text{N}^{15}\text{N}$ a single high-order spin system which includes the ^{15}N nuclei and all aromatic protons. The coupling constants of a given ^{15}N atom to an aromatic proton of the same ring can be estimated from the average coupling constants of pyridine and pyridinium [38] assembled in Table 4. We note that only the coupling constants $J(\text{N}1, \text{H}1)$ and $J(\text{N}1, \text{H}6)$ should be larger than the experimental line width of about 3 Hz. Couplings between nitrogen atoms and aromatic protons in different rings will be even smaller and can be safely neglected for our purposes.

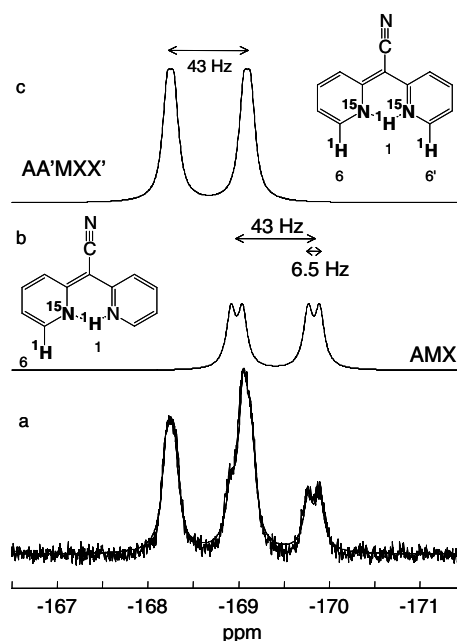


Fig. 1. ^{15}N NMR spectrum without ^1H decoupling of a solution of **1** in CD_2Cl_2 at 183 K. (a) Superimposed experimental and simulated spectra. (b and c) Calculated subspectra arising from two the isotopologs **1**- $^{14}\text{N}^{15}\text{N}$ and **1**- $^{15}\text{N}^{15}\text{N}$.

Table 4
 $^nJ(^{15}\text{N}-^1\text{H})$ coupling constants in pyridine and pyridinium [38] [Hz]

	$^1J(\text{N},\text{H})$	$^2J(\text{N},\text{H}_2)$	$^3J(\text{N},\text{H}_3)$	$^4J(\text{N},\text{H}_4)$
Pyridine ^a	0	−10.58	−1.52	[0.22]
Pyridinium	−90.5	−3.01	−3.98	[0.69]
Pyridine–pyridinium ^b	−45.3	−6.8	−2.8	[0.46]

^a Averaged values of three data sets from Ref. [38].

^b Averaged values for pyridine and pyridinium calculated using Eq. (1).

It follows that the spin system of $1\text{-}^{14}\text{N}^{15}\text{N}$ reduces to an AMX spin system and of $1\text{-}^{15}\text{N}_2$ to an AA'MXX' spin system as illustrated in Fig. 1. The signal of $1\text{-}^{14}\text{N}^{15}\text{N}$ consists then of a doublet of doublets, from which the coupling constants $J(\text{N}1,\text{H}1) = 43\text{ Hz}$ and $J(\text{N}1,\text{H}6) = 6.5\text{ Hz}$ are obtained which represent in first approximation half of the intrinsic couplings. Besides these parameters, only the ^{15}N chemical shift of $1\text{-}^{14}\text{N}^{15}\text{N}$ is obtained (−169.4 ppm).

The signal of $1\text{-}^{15}\text{N}_2$ seems to be deceptively simple. The splitting of the coupling with H6 is no longer observed although this coupling is not suppressed. As the spin system is of the type AA'MXX', where A, A' = ^{15}N , M = H1, X, X' = H6, H6', it is characterized by the six coupling constants

- $J(\text{A},\text{M}) = J(\text{A}',\text{M}) = ^1J(\text{N}1,\text{H}1) = ^1J(\text{N}1',\text{H}1) = 43\text{ Hz}$
- $J(\text{A},\text{X}) = J(\text{A}',\text{X}') = ^2J(\text{N}1,\text{H}6) = ^2J(\text{N}1',\text{H}6') = 6.5\text{ Hz}$
- $J(\text{A},\text{A}') = ^{2h}J(\text{N}1,\text{N}1') \equiv J(\text{N},\text{N})$
- $J(\text{A},\text{X}') = J(\text{A}',\text{X}) = ^{4h}J(\text{N}1,\text{H}6') = ^{4h}J(\text{N}1',\text{H}6)$
- $J(\text{M},\text{X}) = J(\text{M},\text{X}') = ^3J(\text{H}1,\text{H}6) = ^3J(\text{H}1,\text{H}6')$
- $J(\text{X},\text{X}') = ^{5h}J(\text{H}6,\text{H}6')$

The first two couplings are already known from the ^{15}N NMR signal of $1\text{-}^{14}\text{N}^{15}\text{N}$. The last three couplings refer to nuclei in different rings and can be neglected in first approximation. Thus, only the value of the NN-coupling $J(\text{N},\text{N})$ remains as important parameter. If $J(\text{N},\text{N})$ were zero, the spin system would separate into two AMX spin systems, leading to a similar ^{15}N line shape as found for $1\text{-}^{14}\text{N}^{15}\text{N}$. Assuming a value of 10 Hz leads to the calculated line shape depicted in Fig. 1c. Unfortunately, the error of this value is substantial, i.e. about $\pm 5\text{ Hz}$. Therefore, in order to achieve higher accuracy of $J(\text{N},\text{N})$, we applied an indirect method, using ^{13}C NMR as described in the next section.

On the other hand, the simulation of the spectra in Fig. 1 gave two further important information. Firstly, we obtained the effect of substituting ^{14}N for ^{15}N in a neighboring ring on the ^{15}N chemical shift of a given nitrogen atom. This shift is about 1 ppm. Secondly, the calculated subspectra in Fig. 1 exhibit the relative intensities 0.375 and 0.625. From these values it follows that the sample was composed of 45% of non-labeled $1\text{-}^{14}\text{N}_2$, 30% of mono-labeled $1\text{-}^{14}\text{N}^{15}\text{N}$ and 25% of doubly labeled $1\text{-}^{15}\text{N}_2$.

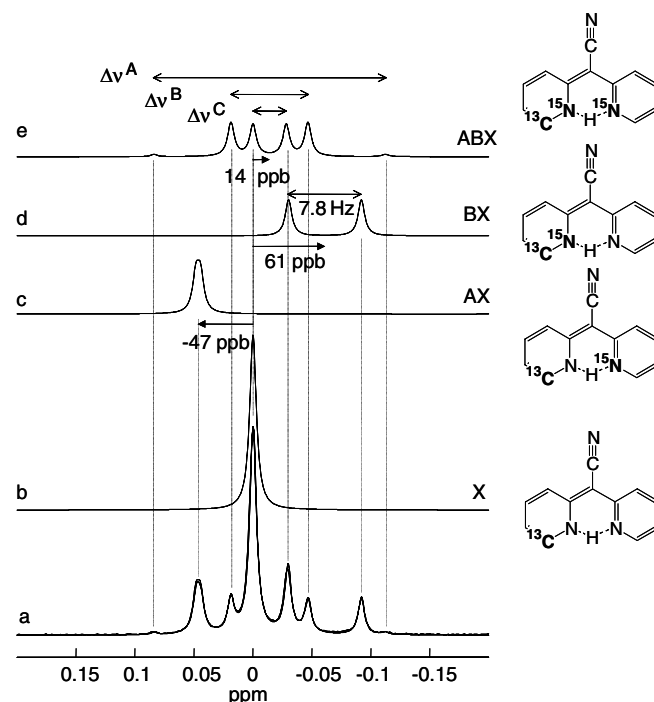


Fig. 2. $^{13}\text{C}\{^1\text{H}\}$ NMR signal at 139.2 ppm, belonging to the C6 nucleus. (a) Experimental and simulated signals; (b–e) simulated subsignals arising from three different isotopomers $1\text{-}^{14}\text{N}_2$, $1\text{-}^{14}\text{N}^{15}\text{N}$, and $1\text{-}^{15}\text{N}_2$. Measurement was performed in CDCl_3 at 213 K. The chemical shift of the line arising from $1\text{-}^{14}\text{N}_2$ was set to zero.

3.3. ^{13}C NMR spectroscopy of **1**

The natural abundance ^{13}C NMR spectrum of **1** consisting of the above-mentioned isotopic mixture was recorded using ^1H decoupling which simplifies the spin systems considerably. The ^{13}C signals of positions 6 and 2 are depicted in Figs. 2 and 3, as well as subspectra of the different isotopologs calculated as described below. Because of fast ^{14}N quadrupole relaxation all couplings between ^{13}C and ^{14}N atoms are removed. Thus, an isotopolog of the type $1\text{-}^{14}\text{N}^{14}\text{N}^{13}\text{C}$ represents effectively a single spin system labeled as X in Figs. 2 and 3b, giving rise to singlets. On the other hand, an isotopolog of the type $1\text{-}^{14}\text{N}^{15}\text{N}^{13}\text{C}$ constitutes an effective two-spin system AX or BX as illustrated in Figs. 2c, d and 3c, d, giving rise to doublets with different splittings $J(^{13}\text{C}, ^{15}\text{N})$. Note that the coupling across the hydrogen bond is not resolved in Fig. 2c.

Finally, isotopologs of the type $1\text{-}^{15}\text{N}^{15}\text{N}^{13}\text{C}$ constitute high-order three-spin systems of the type ABX as illustrated in Figs. 2e and 3e. In order to understand how the coupling constant $J(\text{N},\text{N})$ across the hydrogen bond is obtained by line shape analysis let us discuss the ABX-type spectra in analytical form as described by Dischler et al. [39]. The X-part of an ABX spin system consists of three line pairs of unequal intensity separated by the line splittings

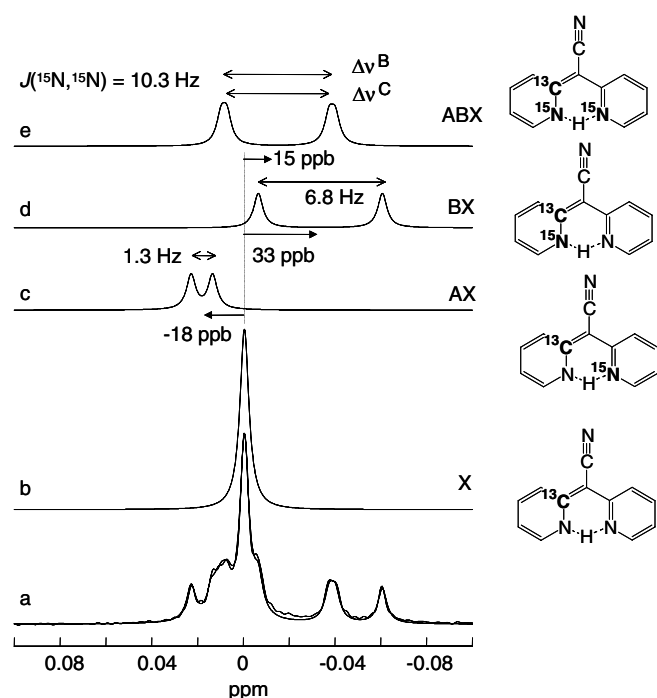


Fig. 3. $^{13}\text{C}\{^1\text{H}\}$ NMR signal at 155.2 ppm, belonging to the C2 nucleus. (a) Experimental and simulated signals; (b–e) simulated subsignals arising from three different isotopomers $1\text{-}^{14}\text{N}_2$, $1\text{-}^{14}\text{N}^{15}\text{N}$, and $1\text{-}^{15}\text{N}_2$. Measurement was performed in CDCl_3 at 213 K. The chemical shift of the line arising from $1\text{-}^{14}\text{N}_2$ was set to zero.

$$\Delta\nu^A = 2 \left\{ \sqrt{0.25J_{AB}^2 + (0.5d + 0.25(J_{AX} - J_{BX}))^2} + \sqrt{0.25J_{AB}^2 + (0.5d - 0.25(J_{AX} - J_{BX}))^2} \right\} \quad (2)$$

$$\Delta\nu^B = |J_{AX} + J_{BX}| \quad (3)$$

$$\Delta\nu^C = \left| 2 \left\{ \sqrt{0.25J_{AB}^2 + (0.5d + 0.25(J_{AX} - J_{BX}))^2} - \sqrt{0.25J_{AB}^2 + (0.5d - 0.25(J_{AX} - J_{BX}))^2} \right\} \right| \quad (4)$$

illustrated in Fig. 2e. Here, $J_{AB} = J(\text{A}, \text{B})$, $J_{AX} = J(\text{A}, \text{X})$, and $J_{BX} = J(\text{B}, \text{X})$.

These splittings do not depend only on the coupling constants but also on the quantity

$$d = |\Delta| \nu_X \times 10^{-6} \text{ Hz}, \quad (5)$$

Table 5
 $^{13}\text{C}\{^1\text{H}\}$ NMR data of **1** derived from measurements at 213 K using CDCl_3 as solvent

	Observable parameters at 11.7 T	Results obtained from the analysis
$^{13}\text{C6}\{^1\text{H}\}$ signal at 139.2 ppm	$\Delta\nu^A = 24.6 \text{ Hz}$ $\Delta\nu^B = 8.1 \text{ Hz}$ $\Delta\nu^C \sim 3.7 \text{ Hz}$ $J_{1,6} = {}^1J(^{13}\text{C}, ^{15}\text{N}) = 7.8 \text{ Hz}$	$J_{1,1'} = J(\text{N}, \text{N}) = \mathbf{10.3 \text{ Hz}}$ $J_{1,6} = {}^1J(\text{C6}, \text{N1}) = -7.8 \text{ Hz}$ $J_{1',6} = {}^3hJ(\text{C6}, \text{N1}') + {}^5J(\text{C6}, \text{N1}')^a \approx {}^3hJ(\text{C6}, \text{N1}') = -0.5 \text{ Hz}$ ${}^1\Delta\text{N}(\text{C6}) = \pm 0.05 \text{ ppm}$
$^{13}\text{C2}\{^1\text{H}\}$ signal at 155.2 ppm	$\Delta\nu^A$ – not observed $\Delta\nu^B \sim 6.4 \text{ Hz}$ $\Delta\nu^C \sim 5.7 \text{ Hz}$	$J_{1,1'} = J(\text{N}, \text{N}) = \mathbf{10.3 \text{ Hz}}$ $J_{1,2} = {}^1J(\text{C2}, \text{N1}) = -6.8 \text{ Hz}$ $J_{1',2} = {}^3hJ(\text{C2}, \text{N1}') + {}^3J(\text{C2}, \text{N1}')^a = +1.3 \text{ Hz}$ ${}^1\Delta\text{N}(\text{C2}) = \pm 0.1 \text{ ppm}$

Bold values indicates most important parameters measured.

^a Two ways of propagation of the J coupling are possible (across hydrogen bridge and along the molecular backbone).

where ν_X represents the Larmor frequency of X and Δ the chemical shift difference between A and B in ppm. As $\text{A}, \text{B} = {}^{15}\text{N}$ and $\text{X} = {}^{13}\text{C}$, it follows that $\Delta = \Delta^{15}\text{N}\{^{13}\text{C}\}$ is the difference of the chemical shifts of the two ${}^{15}\text{N}$ nuclei, one bound to ${}^{12}\text{C}$ and the other to ${}^{13}\text{C}$. Thus, in Eqs. (2)–(5) there are four unknowns, i.e. $J(\text{A}, \text{B})$, $J(\text{A}, \text{X})$, $J(\text{B}, \text{X})$, and d but only three measurable line splittings. As proposed previously, the missing parameter can be extracted from two $^{13}\text{C}\{^1\text{H}\}$ spectra measured at two different magnetic fields as the parameter d is field dependent [8,18]. This method makes it possible to obtain the coupling constant $J(\text{N}, \text{N})$ analytically from resonance frequencies.

Studies at two magnetic fields are, however, not always available. In order to get additional information, needed for the solution of Eqs. (2)–(5), we propose an alternative method, which does not require two different fields. This method is based on the analysis of overlapping signals of the isotopologs $1\text{-}^{15}\text{N}_2$, $1\text{-}^{14}\text{N}^{15}\text{N}$ and $1\text{-}^{14}\text{N}_2$ present in a partially labeled sample as illustrated in Figs. 2 and 3. Neglecting isotope effects on coupling constants, it follows that the coupling constants $J(\text{A}, \text{X})$ and $J(\text{B}, \text{X})$ can be extracted from the doublets in Fig. 2c and d for the carbon in position 6, and in Fig. 3c and d for the carbon in position 2. Thus, only $J(\text{A}, \text{B})$ and d needed to be determined from the two of the splittings $\Delta\nu^A$, $\Delta\nu^B$, $\Delta\nu^C$. Thus, we were able to determine $J(\text{N}, \text{N})$ in an analytical way. The results are presented in Table 5. From both ^{13}C signals we obtained the same value of 10.3 Hz. Finally, we used these parameters to simulate all subspectra in Figs. 2 and 3 and their sum which reproduces well the experimental spectra.

The ^{13}C and ${}^{15}\text{N}$ NMR data of **1** measured in this study are included in Table 5. It contains chemical shifts, coupling constants, as well as ${}^{15}\text{N}/{}^{14}\text{N}$ and ${}^{13}\text{C}/{}^{12}\text{C}$ isotope effects on chemical shifts.

4. Discussion

4.1. Isotopic labeling scheme and indirect ^{13}C determination of scalar coupling between equivalent ${}^{15}\text{N}$ nuclei

We have used liquid-state ^1H , ^{13}C , and ${}^{15}\text{N}$ NMR to study the scalar coupling in ${}^{15}\text{N}$ labeled bis-(2-pyridyl)-acetonitrile (**1**). Due to fast degenerate proton tautomerism

the hydrogen bond proton in **1** exhibits a coupling with both nitrogen nuclei N1 and N1', characterized by a coupling constant of -43 Hz. As both nitrogen nuclei are equivalent, the NN coupling constant $J(\text{N},\text{N})$ across the hydrogen bridge cannot be measured directly. However, the occurrence of scalar coupling between nitrogen and hydrogen H6 (i.e. $J(\text{N1},\text{H6}) = 6.5$ Hz) lifts the magnetic equivalence of nitrogen nuclei. Thus, $J(\text{N},\text{N})$ could be obtained by ^{15}N NMR in the absence of ^1H decoupling. However, the accuracy of this procedure is poor.

In previous papers [8,18], some of us presented an indirect method of determination of $J(\text{N},\text{N})$ by ^{13}C NMR at two different Larmor frequencies. Here, used an isotopic labeling strategy which allows one to obtain the desired constant in a single experiment. The strategy consists simply of partial ^{15}N -labeling giving rise to the occurrence of mono and doubly ^{15}N labeled isotopologs. The former form an AX or BX spin system, and the latter an ABX spin system where A and B represent nitrogen atoms and X a coupled ^{13}C nucleus at natural abundance. The presence of the mono ^{15}N -labeled molecules in the sample provides the coupling constants $J(\text{A},\text{X})$ and $J(\text{B},\text{X})$ needed to extract $J(\text{A},\text{B})$ from the X part of the ABX spin system. The analysis of two different carbon signals, C6 and C2 (see Scheme 1) produced the same value for $J(\text{N},\text{N}) = 10.3 \pm 0.5$ Hz in **1**, confirming the reliability of this method.

The N,N-coupling constant pathway may propagate across the intramolecular hydrogen bond or through four intramolecular bonds of the molecular backbone. We expect the contribution of the latter to be negligible. A literature check did not reveal a measured coupling constant of the type $^4J(\text{N},\text{N})$.

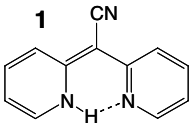
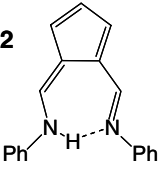
4.2. Implications for hydrogen bond research

In the remainder of this section we will discuss the implications of our findings for hydrogen bond research. Especially interesting is the comparison of bis-(2-pyridyl)-acetonitrile **1** with the fulvenalimine **2** (Scheme 1) which represent both neutral H-chelates. Various parameters relevant for their hydrogen bonds are summarized in Table 6.

For H-chelates it is often difficult to characterize their hydrogen bond strength, as an equilibrium between open and closed forms is not observable. Traditionally, IR spectroscopy has been an important tool to study hydrogen bond strength. However, as stated already by Müller-Westhoff [29], the IR spectra of **2** and its derivatives gives rise to broad unstructured NH-stretching bands in the region between 3000 and 2500 cm^{-1} which presents little information. According to the classification of Novak [40], these frequencies correspond to hydrogen bonds of medium strength. This is confirmed by the X-ray crystallographic N...N distance of **2** which was found to be 2.791 Å [29]. Unfortunately, a crystal structure of **1** is not available. However, 6,6'-substituted symmetric derivatives exhibit a significantly shorter N...N distance of about 2.65 Å. The N...H distances cannot be obtained by X-ray crystallogra-

Table 6

N–H...N geometries calculated using DFT methods and some relevant X-ray crystallographic and NMR data of **1** and **2**

	1	2
		
$R_{\text{NN}}/\text{\AA}$ (DFT)	2.603	2.723
$R_{\text{NN}}/\text{\AA}$ (X-ray structure)	2.65 ^a	2.791 ^b
$r_{\text{NH}}/\text{\AA}$	1.051	1.057
$r_{\text{H...N}}/\text{\AA}$	1.696	1.705
$\angle \text{N-H...N}/^\circ$ (DFT)	141.64	160.25
$\angle \text{N-H...N}/^\circ$ (X-ray structure)	≈ 137	≈ 155
$\angle \text{CCNH}/^\circ$	0.00	-0.85
$\angle \text{CCN...H}/^\circ$	0.00	2.12
$q_1/\text{\AA}$	0.323	0.324
$q_2/\text{\AA}$	2.747	2.762
$\delta(^1\text{H})/\text{ppm}$	16.2 ^c	15.6 ^d
$J(\text{N},\text{H1})/\text{Hz}$	-43^c	-40.8^d
$J(\text{N},\text{N})/\text{Hz}$	10.3^c	10.6^d

Bold values indicates most important parameters measured.

^a Derivatives of **1** with two equal substituents in 6-position according to Refs. [24,27,28].

^b Ref. [29].

^c 213/183 K, $\text{CD}_2\text{Cl}_2/\text{CDCl}_3$, this study.

^d RT, CDCl_3 [8].

phy, and the hydrogen bond angles only in approximation. Nevertheless, with 160° the H-bond in **2** is more linear than in **1** which exhibits only an angle of 140° (Table 6). Finally, we note that **1** is planar whereas the NH and the H...N axes of **2** are located slightly outside the molecular plane defined by the adjacent C...C axes (Table 6).

Although the hydrogen bond geometries of **1** and **2** are different, we find that the ^1H chemical shifts of the H-bonded protons are very similar, i.e. 16.2 and 15.6 ppm. The tautomerism averaged coupling constants $J(\text{N},\text{H})$ of 43 and 40 Hz indicate a slightly stronger bond in **2**, in contrast to the chemical shift values. Most surprising for us was the finding that the N...N coupling $J(\text{N},\text{N})$ of **2** is only slightly larger than of **1**: 10.6 Hz for **2** and 10.3 Hz for **1** which are almost the same within the margin of error.

In order to elucidate the origin of the similarity of the N...N couplings in both compounds we needed more information about the hydrogen bond geometries of both compounds. Therefore, we carried out DFT calculations of **1** and **2**, using the Gaussian 98 set of programs [41] at the B3PW91/6-31+G** level of density functional theory (DFT) [42]. We are aware that the results obtained refer to the equilibrium geometries, i.e. they do not take into account anharmonic vibrational averaging nor solute-solvent interactions.

The calculated geometries of the N–H...N bridges are included in Table 6. The calculated N...N distances of **1** and **2** are about 0.06 Å shorter than the crystallographic

values, but this deviation is not large as the shorter N...N distance in **1** as compared to **2** is well reproduced. The hydrogen bond angles are also of the order found by X-ray crystallography.

A surprising result was, however, the finding that the short NH distances in **1** and **2** are almost the same. The same is true for the long H...N distances, and, therefore, also for the intrinsic hydrogen bond coordinates

$$q_1 = 1/2(r_{\text{NH}} - r_{\text{H...N}}) \quad \text{and} \quad q_2 = r_{\text{NH}} + r_{\text{H...N}} \quad (6)$$

listed in Table 6. For linear H-bonds q_1 represents the deviation of the proton from the H-bond center and q_2 the heavy atom distance. As has been shown in various papers [7,43–45], r_{NH} correlates with $r_{\text{H...N}}$ and hence q_1 with q_2 . This finding confirms the hypothesis made previously by some of us [7] that the $J(\text{N},\text{N})$ coupling constants correlate rather with q_1 and hence with q_2 , than with the N...N distance.

5. Conclusions

We conclude that the indirect determination by ^{13}C NMR of $^2hJ(^{15}\text{N}, ^{15}\text{N}) \equiv J(\text{N},\text{N})$ coupling constants across $^{15}\text{N}\text{—H}\cdots^{15}\text{N}$ hydrogen bonds exhibiting chemically equivalent nitrogen atoms is greatly improved by measurements performed on a mixture of singly and doubly ^{15}N labeled isotopologs. The application of this method to the six-membered H-chelate bis-(2-pyridyl)-acetonitrile (**1**) and the comparison with the seven-membered H-chelate fulvenaldimine **2** (Scheme 1) support the idea that the values of $J(\text{N},\text{N})$ are correlated with the sum of the short and the long NH distances rather than with the N...N distance. A remaining puzzle are the values of $J(\text{N},\text{N})$ for proton sponges [18,21] which are significantly smaller than those of **1** and **2** (Scheme 1), although the hydrogen bonds are substantially stronger. In order to solve this puzzle, further experimental and theoretical work will be necessary.

Acknowledgments

This work has been supported by the Deutsche Forschungsgemeinschaft and the Fonds der Chemischen Industrie, Frankfurt.

References

- [1] (a) S.N. Smirnov, N.S. Golubev, G.S. Denisov, H. Benedict, P. Schah-Mohammed, H.H. Limbach, *J. Am. Chem. Soc.* 118 (1996) 4094–4101; (b) H.H. Limbach, M. Pietrzak, S. Sharif, P.M. Tolstoy, I.G. Shenderovich, S.N. Smirnov, N.S. Golubev, G.S. Denisov, *Chem. Eur. J.* 10 (2004) 5195–5204.
- [2] I.G. Shenderovich, S.N. Smirnov, G.S. Denisov, V.A. Gindin, N.S. Golubev, A. Dunger, R. Reibke, S. Kirpekar, O.L. Malkina, H.H. Limbach, *Ber. Bunsenges. Phys. Chem.* 102 (1998) 422–428.
- [3] A.J. Dingley, S. Grzesiek, *J. Am. Chem. Soc.* 120 (1998) 8293–8297.
- [4] S. Grzesiek, F. Cordier, V. Jaravine, M. Barfield, *Prog. Nucl. Magn. Reson. Spectrosc.* 45 (2004) 275–300.
- [5] I.G. Shenderovich, A.P. Burtsev, G.S. Denisov, N.S. Golubev, H.H. Limbach, *Magn. Res. Chem.* 39 (2001) S91–S99.
- [6] J.E. Del Bene, J. Elguero, *J. Phys. Chem.* 110 (2006) 7496–7502.
- [7] H. Benedict, I.G. Shenderovich, O.L. Malkina, V.G. Malkin, G.S. Denisov, N.S. Golubev, H.H. Limbach, *J. Am. Chem. Soc.* 122 (2000) 1979–1988.
- [8] M. Pietrzak, H.H. Limbach, M. Pérez-Torralba, D. Sanz, R.M. Claramunt, J. Elguero, *Magn. Reson. Chem.* 39 (2001) S100–S108.
- [9] N.S. Golubev, I.G. Shenderovich, S.N. Smirnov, G.S. Denisov, H.H. Limbach, *Chem. Eur. J.* 5 (1999) 492–497.
- [10] I.G. Shenderovich, P. Tolstoy, N.S. Golubev, S.N. Smirnov, G.S. Denisov, H.H. Limbach, *J. Am. Chem. Soc.* 125 (2003) 11710–11720.
- [11] A.J. Dingley, J.E. Masse, R.D. Peterson, M. Barfield, J. Feigon, S. Grzesiek, *J. Am. Chem. Soc.* 121 (1999) 6019–6027.
- [12] F. Cordier, S. Grzesiek, *J. Am. Chem. Soc.* 121 (1999) 1601–1602.
- [13] F. Cordier, M. Rogowski, S. Grzesiek, A. Bax, *J. Magn. Reson.* 140 (1999) 510–512.
- [14] K. Pervushin, A. Ono, C. Fernandez, T. Szyperski, M. Kainosho, K. Wüthrich, *Proc. Natl. Acad. Sci. USA* 95 (1998) 14147–14151.
- [15] G. Cornilescu, B.E. Ramirez, M.K. Frank, G.M. Clore, A.M. Gronenborn, A. Bax, *J. Am. Chem. Soc.* 121 (1999) 6275–6279.
- [16] G. Cornilescu, J.S. Hu, A. Bax, *J. Am. Chem. Soc.* 121 (1999) 2949–2950.
- [17] C. Scheurer, R. Brüschweiler, *J. Am. Chem. Soc.* 121 (1999) 8661–8662.
- [18] M. Pietrzak, J. Wehling, H.H. Limbach, N.S. Golubev, C. López, R.M. Claramunt, J. Elguero, *J. Am. Chem. Soc.* 123 (2001) 4338–4339.
- [19] V.A. Ozeryanskii, A.F. Pozharskii, A.J. Bienko, W. Sawka-Dobrowolska, L. Sobczyk, *J. Phys. Chem. A* 109 (2005) 1637–1642 (and references cited therein).
- [20] S. Berger, *J. Magn. Reson.* 66 (1986) 555–557.
- [21] G.C. Lloyd-Jones, J.N. Harvey, P. Hodgson, M. Murray, R.L. Woodward, *Chem. Eur. J.* 9 (2003) 4523–4535.
- [22] N. Sperber, D. Papa, E. Schwenk, M. Sherlock, N.J. Bloomfield, *J. Am. Chem. Soc.* 73 (1951) 3856–3858.
- [23] (a) R. Griebel, *Ber. Bunsenges. Phys. Chem.* 84 (1980) 84–91; (b) R. Griebel, *Ber. Bunsenges. Phys. Chem.* 84 (1980) 919–925; (c) G.E. Scheibe, E. Daltrozzo, O. Wörz, *Z. Physik. Chem.* 64 (1969) 97–114.
- [24] I.O. Fritsky, R. Ott, R. Kramer, *Angew. Chem. Int. Ed. Engl.* 39 (2000) 3255–3258.
- [25] E. Daltrozzo, *Habilitationsschrift*, TU München, 1971.
- [26] E. Daltrozzo, *Proc. XX. Coll. Spectr. Internat., Invited Lectures II*, Prag, 1977, pp. 151–174.
- [27] G.R. Newkome, Y.J. Joo, D.W. Evans, S. Pappalardo, F.R. Fronczek, *J. Org. Chem.* 53 (1988) 786–790.
- [28] G.R. Newkome, Y.J. Joo, K.J. Theriot, F.R. Fronczek, *J. Am. Chem. Soc.* 108 (1986) 6074–6075.
- [29] (a) U. Mueller-Westerhoff, *J. Am. Chem. Soc.* 92 (1970) 4849–4855; (b) H.L. Ammon, U. Mueller-Westerhoff, *Tetrahedron* 30 (1974) 1437–1443.
- [30] K.N. Trueblood, in: A. Domenicano, I. Hargittai (Eds.), “Accurate Molecular Structures, Their Determination and Importance”, Oxford University Press, 1992, p. 200 (Chapter 8).
- [31] (a) M. Barfield, A.J. Dingley, J. Feigon, S. Grzesiek, *J. Am. Chem. Soc.* 123 (2001) 4014–4022; (b) E. Grech, J. Klimkiewicz, J. Nowicka-Scheibe, M. Pietrzak, W. Schilf, A.F. Pozharskii, V.A. Ozeryanskii, S. Bolvig, J. Abildgaard, P.E. Hansen, *J. Mol. Struct.* 615 (2002) 121–140.
- [32] (a) M.R. Stetten, R. Schoenheimer, *J. Biol. Chem.* 153 (1944) 113–132; (b) H. Pechmann, *Ann. Chem.* 261 (1891) 151–172; (c) H. Pechmann, W. Welsh, *Ber. Chem. Ges.* 17 (1884) 2384–2390; (d) H. Pechmann, O. Baltzer, *Ber. Chem. Ges.* 24 (1891) 3144–3153; (e) R.A. Coburn, G.O. Dudek, *J. Phys. Chem.* 72 (1968) 1177–1181.
- [33] F.M. Saidova, G.P. Gorbunova, *USSR Fiz. khim. Issled. Sintetich. i Prirod. Soedin.*, Samarkand, 1980, pp. 68–74 (From Ref. Zh. Khim., 1981, Abstr. No. 11Zh204.).

- [34] A.L. Borror, A.F. Haeberer, *J. Org. Chem.* 30 (1965) 243–246.
- [35] W. Sulger, Ph. D. Thesis, University of Konstanz, 1981 (For carrying-out these very syntheses of bis-(2-pyridyl)-acetonitriles, we are much obliged to M. Neureiter.).
- [36] (a) H. Gehring, Master Thesis, University of Konstanz, 1995.;
(b) H. Gehring, Ph.D. Thesis, University of Konstanz, ISBN 3-930803-47-X, 1998;
(c) H. Gehring, E. Daltrozzi, *Helv. Chim. Acta* 81 (1998) 236–250.
- [37] K. Klemm, H. Schaefer, E. Daltrozzi, *Chem. Ber.* 112 (1979) 484–495.
- [38] G.J. Martin, M.L. Martin, J.P. Gouesnard, ¹⁵N NMR Spectroscopy, Springer-Verlag, Berlin, Heidelberg, New York, 1981 (p. 224).
- [39] (a) B. Dischler, *Angew. Chem.* 78 (1966) 653–663;
(b) J.W. Emsley, J. Feeney, L.H. Sutcliffe, *High Resolution Nuclear Magnetic Resonance Spectroscopy*, vol. 1, Pergamon Press, Oxford, 1965, pp. 357–364.
- [40] A. Novak, *Struct. Bonding (Berlin)* 18 (1974) 177–216.
- [41] M.J. Frisch, G.W. Trucks, H.B. Schlegel, G.E. Scuseria, M.A. Robb, J.R. Cheeseman, V.G. Zakrzewski, J.A. Montgomery Jr., R.E. Stratmann, J.C. Burant, S. Dapprich, J.M. Millam, A.D. Daniels, K.N. Kudin, M.C. Strain, O. Farkas, J. Tomasi, V. Barone, M. Cossi, R. Cammi, B. Mennucci, C. Pomelli, C. Adamo, S. Clifford, J. Ochterski, G.A. Petersson, P.Y. Ayalla, Q. Cui, K. Morokuma, D.K. Malick, A.D. Rabuck, K. Raghavachari, J.B. Foresman, J. Cioslowski, J.V. Ortiz, A.G. Baboul, B.B. Stefanov, G. Liu, A. Liashenko, P. Piskorz, I. Komaromi, R. Gomperts, R.L. Martin, D.J. Fox, T.M. Keith, A. Al-Laham, C.Y. Peng, A. Nanayakkara, C. Gonzalez, M. Challacombe, P.M.W. Gill, B. Johnson, W. Chen, M.W. Wong, J.L. Andres, M. Head-Gordon, E.S. Replogle, J.A. Pople, *Gaussian 98, Revision A7*, Gaussian Inc., Pittsburgh, PA, 1998.
- [42] (a) R.G. Parr, W. Yang, *Density Functional Theory of Atoms and Molecules*, Oxford University Press, New York, 1989;
(b) N.H. March, *Electron Density Theory of Atoms and Molecules*, Academic Press, San Diego, CA, 1992.
- [43] T. Steiner, *J. Phys. Chem. A* 102 (1998) 7041–7052.
- [44] H.H. Limbach, M. Pietrzak, H. Benedict, P.M. Tolstoy, N.S. Golubev, G.S. Denisov, *J. Mol. Struct.* 706 (2004) 115–119.
- [45] H.H. Limbach, G.S. Denisov, N.S. Golubev, in: A. Kohen, H.H. Limbach (Eds.), *Isotope Effects in the Biological and Chemical Sciences*, Taylor & Francis, Boca Raton, FL, 2006, pp. 193–230 (Chapter 7, Hydrogen Bond Isotope Effects Studied by NMR).